Detection of damage to building side-walls in the 2011 Tohoku, Japan earthquake using high-resolution TerraSAR-X images

Fumio Yamazaki*[a], Yoji Iwasaki[b], Wen Liu[c], Takashi Nonaka[d], Tadashi Sasagawa[d]

[a] Graduate School of Eng., Chiba University, 1-33 Yayoi-cho, Inage-ku, Chiba, Japan 263-8522;
[b] Chiba Prefectural Government, 1-1 Ichiba-cho, Chuo-ku, Chiba, Japan 260-8667;
[c] JSPS Research Fellow, Tokyo Institute of Technology, 4259 Nagatsuta-cho, Midori-ku, Yokohama, Kanagawa, Japan 226-8502;
[d] Satellite Division, PASCO Co., 4-10-1 Nakano, Nakano-ku, Tokyo, Japan, 164-0001

ABSTRACT

Building damage such as to side-walls or mid-story collapse is often overlooked in vertical optical images. Hence, in order to observe such building damage modes, high-resolution SAR images are introduced considering the side-looking nature of SAR. In the 2011 Tohoku, Japan, earthquake, a large number of buildings were collapsed or severely damaged due to repeated tsunamis. One of the important tsunami effects on buildings is that the damage is concentrated to their side-walls and lower stories. Thus this paper proposes the method to detect this kind damage from the change in layover areas in SAR intensity images. Multi-temporal TerraSAR-X images covering the Sendai-Shiogama Port were employed to detect building damage due to the tsunamis caused by the earthquake. The backscattering coefficients in layover areas of individual buildings were extracted and then, the average value in each layover area was calculated. The average value was seen to decrease in the post-event image due to the reduced backscatter from building side-walls. This example demonstrated the usefulness of high-resolution SAR intensity images to detect severe damage to building side-walls based on the changes of the backscattering coefficient in the layover areas.

Keywords: TerraSAR-X, layover, side-wall, 2011Tohoku earthquake, building damage, tsunami

1. INTRODUCTION

Remote sensing has been recognized as an efficient tool to monitor a wide range of the earth's surface in the normal time and in natural disasters. Damage detection of buildings soon after the occurrence of natural disasters is one of the important topics of satellite remote sensing. A number of studies have been conducted to identify damage situation of individual buildings from high-resolution multi-spectral sensors (e.g. QuickBird, Ikonos, WorldView-2) after damaging earthquakes in the world [1-5]. In these studies, the damage grades of buildings were judged from optical images captured from the vertical direction. Hence the building damages such as mid-story collapse or damage to side-walls were often overlooked because only the upper surfaces of buildings could be seen and thus such types of damage modes were mostly invisible. But it is possible to detect such damage modes by measuring the building heights based on two stereoscopic satellite images taken from slightly different positions at the same time. However, this method requires a total of four images before and after an earthquake to measure the change in building heights, and thus is not so practical in terms of cost efficiency. The present authors [6] have proposed the use of building shadow lengths to detect mid-story collapse from optical satellite images. But this method cannot be applied in detecting damage to building side faces.

Although optical images can easily capture detailed ground surface information, the approach is limited by weather conditions. In contrast, synthetic aperture radar (SAR) sensing is independent of weather and daylight conditions, and thus more suitable for mapping damaged areas promptly. Due to remarkable improvements in radar sensors, high-resolution TerraSAR-X and COSMO-SkyMed SAR images are possible with ground resolution of 1 to 5 m, providing detailed surface information. The damage detection of urban areas using these high-resolution SAR images has become quite popular recently. Comparing the change in pre-event and post-event SAR intensity images, damage detection of buildings has been conducted several researchers [7-10]. Due to the side-looking nature of SAR, the layover of buildings and the multi-bounce of radar among the ground and buildings occur. These phenomena are significant in dense urban areas and then make damage identification of individual buildings difficult. However, if a building stands alone or faces to a wide street, the length of layover indicates the height of the building [11] and the status of its side-wall facing to the

radar illumination direction. Utilizing the change in the backscattering intensity within the layover area of an individual building, this study attempts to detect the damage situation of building side-walls due to the 2011 Tohoku, Japan earthquake and tsunami.

2. THE 2011 TOHOKU, JAPAN EARTHQUAKE AND TERRASAR-X DATA USED

The Mw 9.0 Tohoku earthquake occurred on March 11, 2011, off the Pacific coast of northeastern (Tohoku) Japan, caused gigantic tsunamis, resulting in widespread devastation. The earthquake resulted from a thrust fault on the subduction zone plate boundary between the Pacific and North American plates. According to the GPS Earth Observation Network System (GEONET) at the Geospatial Information Authority (GSI) in Japan, crustal movements with maximums of 5.3 m to the horizontal (southeast) and 1.2 m to the vertical (downward) directions were observed over a wide area [12]. Using pre- and post-event TerraSAR-X (TSX) intensity images, the present authors carried out the estimation of the crustal movements based on an improved pixel-offset method, where the cross-correlation was evaluated for small areas including a non-damaged building and then the average of them were considered to represent the surface displacement [13, 14].

The Tohoku earthquake triggered extremely high tsunamis of up to 40.5 m run-up in Miyako, Iwate Prefecture, and caused huge loss of human lives and destruction of infrastructure. According to the GSI, areas totaling approximately 561 km^2 were flooded by tsunamis following the earthquake [12]. Due to the huge tsunami, about 107 thousands buildings were washed away or collapsed. In this regard, the present authors [10] conducted the extraction of flooded areas due to the tsunami and identified washed-away buildings using the pre- and post-event TSX intensity images. Typical building damages due to the 2011 Tohoku earthquake tsunami in our field survey were shown in Fig. 1. The characteristic building damage by tsunami is that damage was caused to building side-walls or lower parts, which is not the same with damage caused by strong earthquake shaking. We try to detect this kind of damage to building side-walls using the side-looking nature of SAR. The strongest backscattering echoes from the side-walls and double-bounce with the ground may be reduced after this type of damage.

In this study, we focuses on the coastal zone of Tohoku, Japan, as shown in Fig. 2, which was one of the most severely affected areas during the 2011 Tohoku earthquake. Three temporal TSX images taken before and after the earthquake are shown in Fig. 1(a-c), which we used previously for detecting crustal movements [13] and identifying flooded areas [10]. The pre-event image was taken on October 21, 2010 (local time), while the post-event ones were taken on March 13 (two days after the earthquake) and April 4, 2011. There is a 37.31° incidence angle at the center of the images. All the images were captured with HH polarization and in a descending path. The images were acquired in the StripMap mode, and so the azimuth resolution was about 3.3 m while the ground range resolution was about 1.2 m. The images were orthorectified multi-look corrected products (EEC) where the image distortion caused by variable terrain height was compensated for by using a globally available DEM (SRTM). Therefore, they have been resampled and projected to a WGS84 reference ellipsoid with a square pixel size of 1.25 m.

Figure 1. Typical tsunami damage to reinforced concrete and steel-frame buildings observed in our field survey after the 2011 Tohoku earthquake in Onagawa, Minami-Sanriku, and Ohtsuchi towns. The damage was concentrated to side-walls and lower stories of buildings.

(a) 2010/10/21 05:43　　　(b) 2011/03/13 05:43　　　(c) 2011/04/04 05:43　　　(d) TSX's Imaging Area
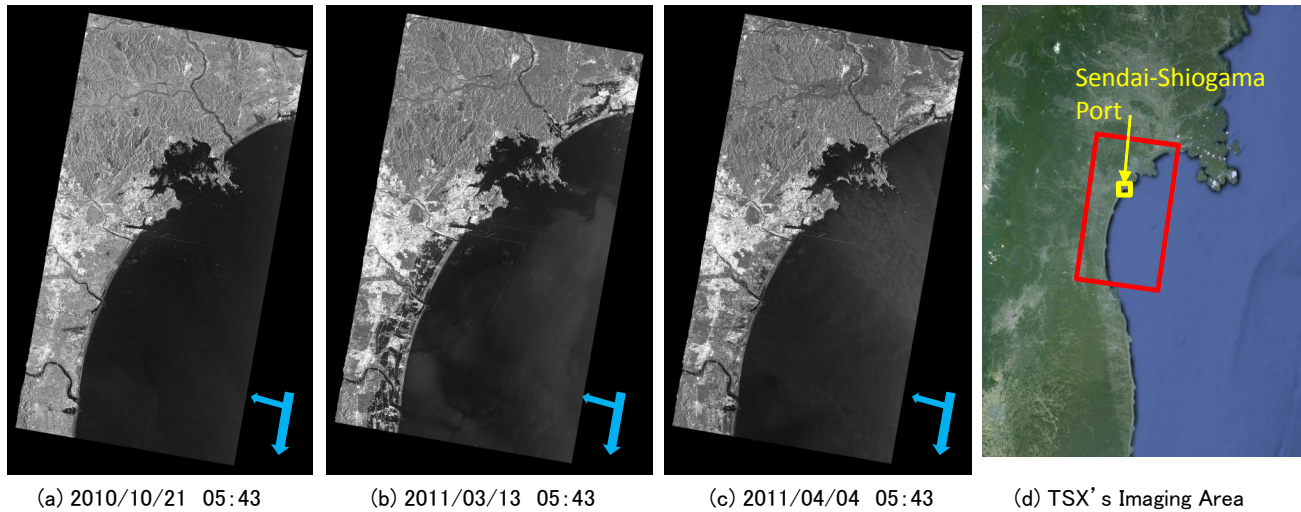
Figure 2. The pre-event TSX image taken on October 21, 2010 (a), the post-event images taken on March 13, 2011 (b) and April 4, 2011 (c), and the TSX's imaging area along the Pacific coast of Tohoku, Japan including the Sendai-Shiogama Port (d).

Two preprocessing approaches were applied to the images. First, the three TSX images were transformed to a Sigma Naught (σ^0) value, which represents the radar reflectivity per unit area in the ground range. After the transformation, the backscattering coefficients of the images were between -30 dB and 30 dB. An enhanced Lee filter [15] was then applied to the original SAR images to reduce the speckle noise, which makes the radiometric and textural aspects less efficient and improves the correlation coefficient between the two images. To minimize any loss of information included in the intensity images, the window size of the Lee filter was set as 3 × 3 pixels.

The displacements caused by crustal movements when the post-event TSX images were taken, were estimated by Liu and Yamazaki [13]. The movement detected in the TSX image on March 13 was 3.11 m to the east and 0.55 m to the south in the Sendai area. Considering that the obtained displacements were approximately 0.3 m larger than GPS ground station records, the pre-event TSX image was manually shifted 2 pixels (2.5 m) to the east in order to match the post-event TSX images.

3. SAR BACKSCATTER CHARACTERISTICS OF BUILDINGS

Backscattering echoes from buildings in very high-resolution (VHR) SAR images include the information on the three-dimensional shapes of buildings. Reconstruction of flat-roof and gable-roof buildings from VHR SAR images were carried out by several researchers [7, 11, 16, 17]. Due to the side-looking geometry of SAR sensors, the backscattering echoes of VHR SAR from a stand-alone building can be shown schematically in Fig. 3.

If a building stands alone on a flat ground, the backscatter from the building shows layover on the ground range. In a usual case, the fringe of the roof-top exhibits strong backscatter (blue arrow **d** in (a) and (c)) and it leans toward to the direction of SAR illumination. The foot fringe of a building also exhibits strong backscatter (blue arrow **b**) due to the double-bounce of radar from the ground and building's side-wall. The backscatter from the building side-wall (blue arrow **c**) together with the double-bounce component, the layover area corresponding to the building side-wall is generally distinguishable in the ground-range SAR intensity image. Thus the height of the building, H, can be calculated from the length of the layover area, L, as

$$H = L \tan \theta \tag{1}$$

where θ is the incidence angle of SAR. A similar geometrical relationship is obtained for a radar shadow area (area f behind the building corresponding to $L'+B$ with B = the building width). If the radar shadow is clearly observed as in Fig. 3 (b), the building height is also estimated by the length of the radar shadow L' as

$$H = L' / \tan \theta \tag{2}$$

In other words, if the height of a building is known, the areas of layover and radar shadow can be estimated on the ground range SAR intensity image. If the lower part of a building side-wall is damaged as represented by Fig. 3 (d), the area of layover due the side-wall ($a+c$) will be reduced or the backscatter intensity of the area will get smaller. The area of radar shadow (f) will also become small for a damaged building.
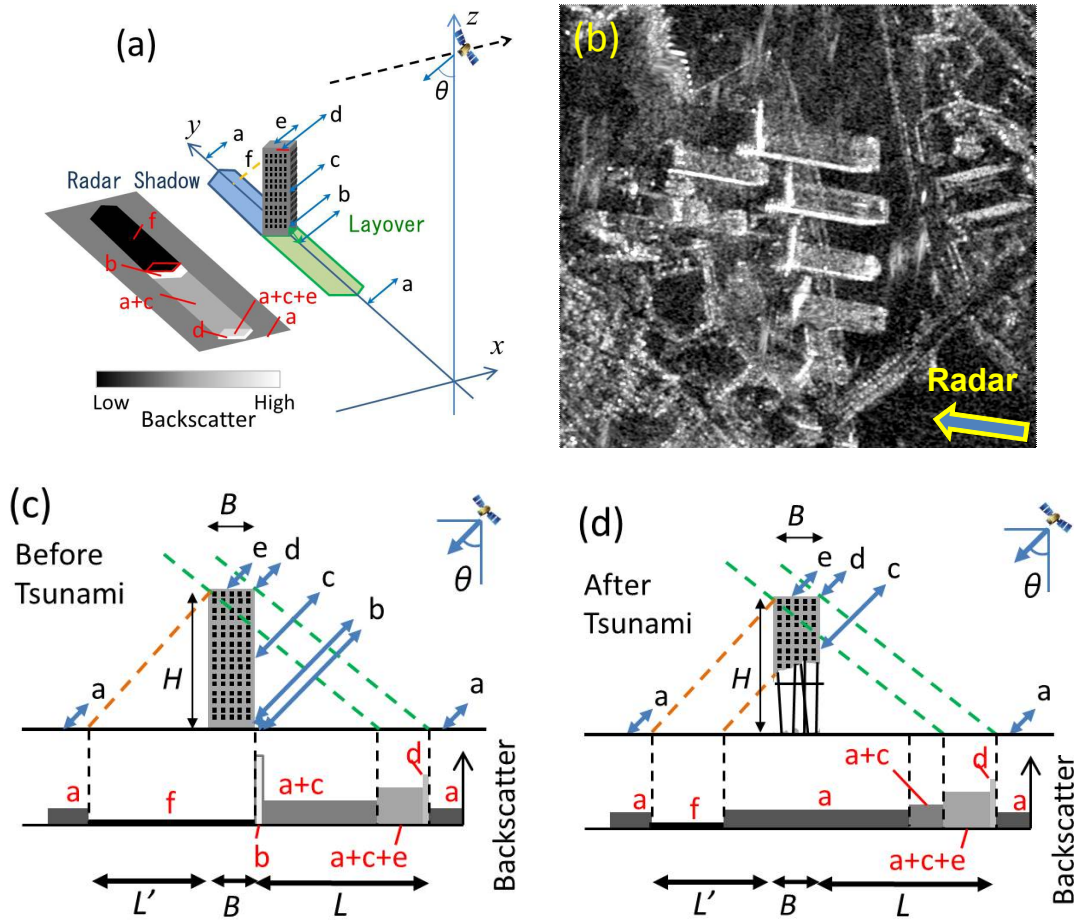
Figure 3. Schematic figure of SAR observation for an ideal tall flat-roof building. 3D layout (a), an actual TSX intensity image for the central Tokyo (b), the amplitude of backscatter from an intact building (c), and the amplitude of backscatter from a damaged building due to tsunami (d).

4. A CASE STUDY FOR SENDAI-SHIOGAMA PORT

The Sendai-Shiogama Port, which was severely hit by the 2011Tohoku earthquake tsunami, was selected as a case study site of building damage detection from SAR images since there were many large buildings and warehouses damaged by the tsunami attack. Figure 4 shows aerial images (adapted from Google Earth) of the Sendai-Shiogama Port and its surroundings after the tsunami attack. Area **A** was located within the tsunami inundation zone and area **B** outside of the zone. Thirteen (13) damaged buildings were extracted from area **A** and thirteen non-damaged ones were selected from area **B**.

In this study, we firstly drew building footprints from the optical images manually. Then the layover areas were determined by shifting the roof-top frames manually. In this stage, the building heights were estimated from the buildings' cast-shadow lengths [6] and the photos in Google Street View. The backscattering coefficients within the estimated layover area for each building were extracted for the pre- and post-event TSX images and their values were used in change detection due to the tsunami attack.
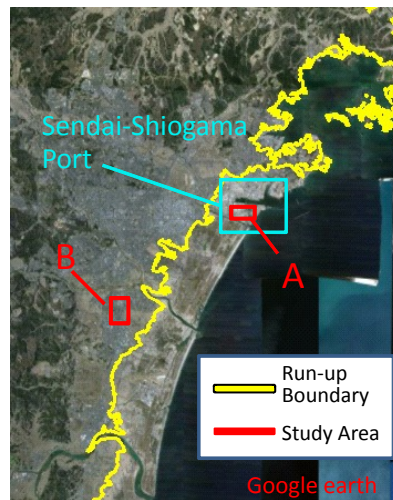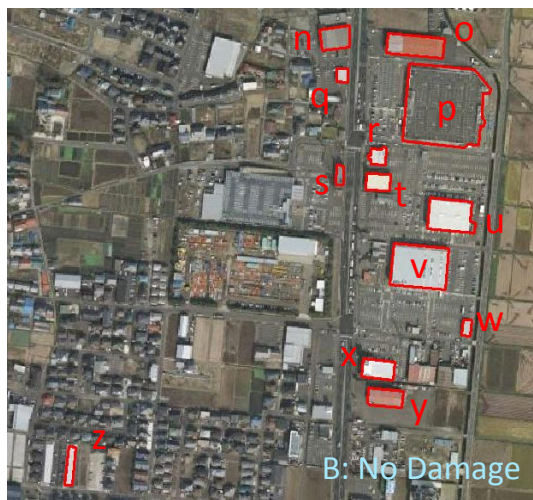
Figure 4. Aerial images of Sendai-Shiogama Port and its surroundings after the tsunami attack. Area **A** within the tsunami inundation zone was severely affected and area **B** was located outside of the zone.
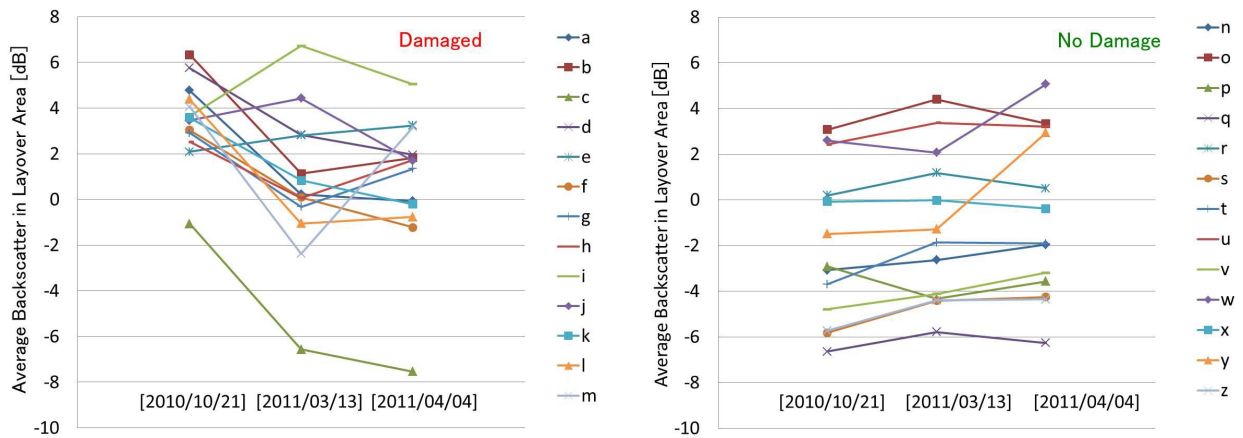
Figure 5. The average value of the backscattering coefficient within the layover area of each building for the 13 damaged buildings in Area **A** and 13 non-damaged buildings in Area **B** at the three time instants of SAR image acquisition.

The average value of the backscattering coefficient within the layover area was calculated for the 13 damaged and 13 non-damaged buildings for the three time instants as shown in Fig. 5. It is observed that for the damaged buildings, the average backscattering coefficient within the layover area tends to be lower in the post-tsunami TSX images while the average value is almost unchanged for the non-damaged buildings.

The difference of the average values of the backscattering coefficients within the layover area of each building before and after the tsunami attack is plotted in Fig. 6 for the 13 damaged buildings (a-m) in Area **A** and 13 non-damaged buildings (n-z) in Area **B**. This figure further confirms the trends seen in Fig. 5. The two post-event TSX data were used to calculate the change in the backscatter within the layover area. The 2011/3/13 image was captured only two days after the tsunami attack, and hence the effect of debris spread on the ground might raise the backscatter there and canceled out the effect of side-wall damage. In the 2011/4/04 image, some debris had been cleared but vehicles and some other objects might exist in the layover area. Due to these possibilities, the difference values are not the same for the two time intervals.
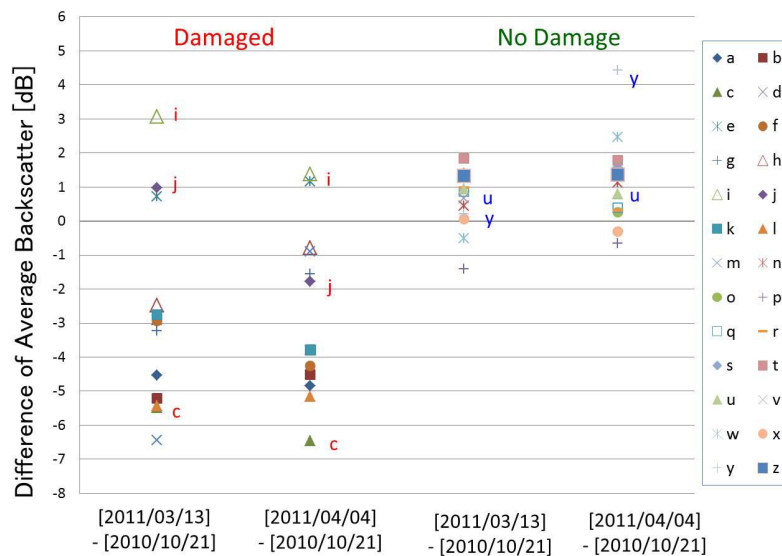
Figure 6. The difference of the average values of the backscattering coefficients within the layover area of each building before and after the tsunami attack for the 13 damaged buildings in Area **A** and 13 non-damaged buildings in Area **B**.

In Fig. 6, the backscatter within the layover area was decreased for most of the damaged buildings. Figure 7 compares the close-up of the TSX images and the optical images of similar acquisition dates for damaged buildings **c**, **i** and **j**. Building **c** suffered from severe tsunami attack on its side-wall and the wall was lost almost completely. Due to this damage situation, the backscatter from the wall as well as the double-bounce component reduced significantly.

Buildings **i** and **j** were outliers of the damaged building category, where the backscatter increased after the tsunami attack. The close-up of these buildings in Fig. 7 shows the spread of debris in their layover areas. Due to relatively small damage to their side-walls and the existence of debris, the backscatter increased in their SAR image on 2011/3/13. The debris was seen being cleared on 2011/4/04, and thus the backscatter of the layover area for building **j** reduced to the level lower than that at the pre-event time. On the contrary, the backscatter for building **i** on 2011/4/04 was still higher than the pre-event time value. This fact may be explained by the exposure of steel frame seen on the side-wall in the ground photo of building **i**. Note that strong radar returns are expected from direct reflection from objects with high dielectric constants, i.e. conductors such as steel [18].

Figure 8 shows the close-up of the TSX images and the optical images for non-damaged buildings **u** and **y**. Building **u** is a typical non-damaged building, where no significant change was seen in its layover area. Building **y** is the only outlier out of the 13 non-damaged buildings, where the increase of backscatter was seen in the TSX image on 2011/4/04. No particular object is seen in the corresponding optical image, but its acquisition date and time was different from that of the TSX image. Since a parking lot exists in the surrounding of the building, parking vehicles might be responsible for this temporary increase of backscatter.
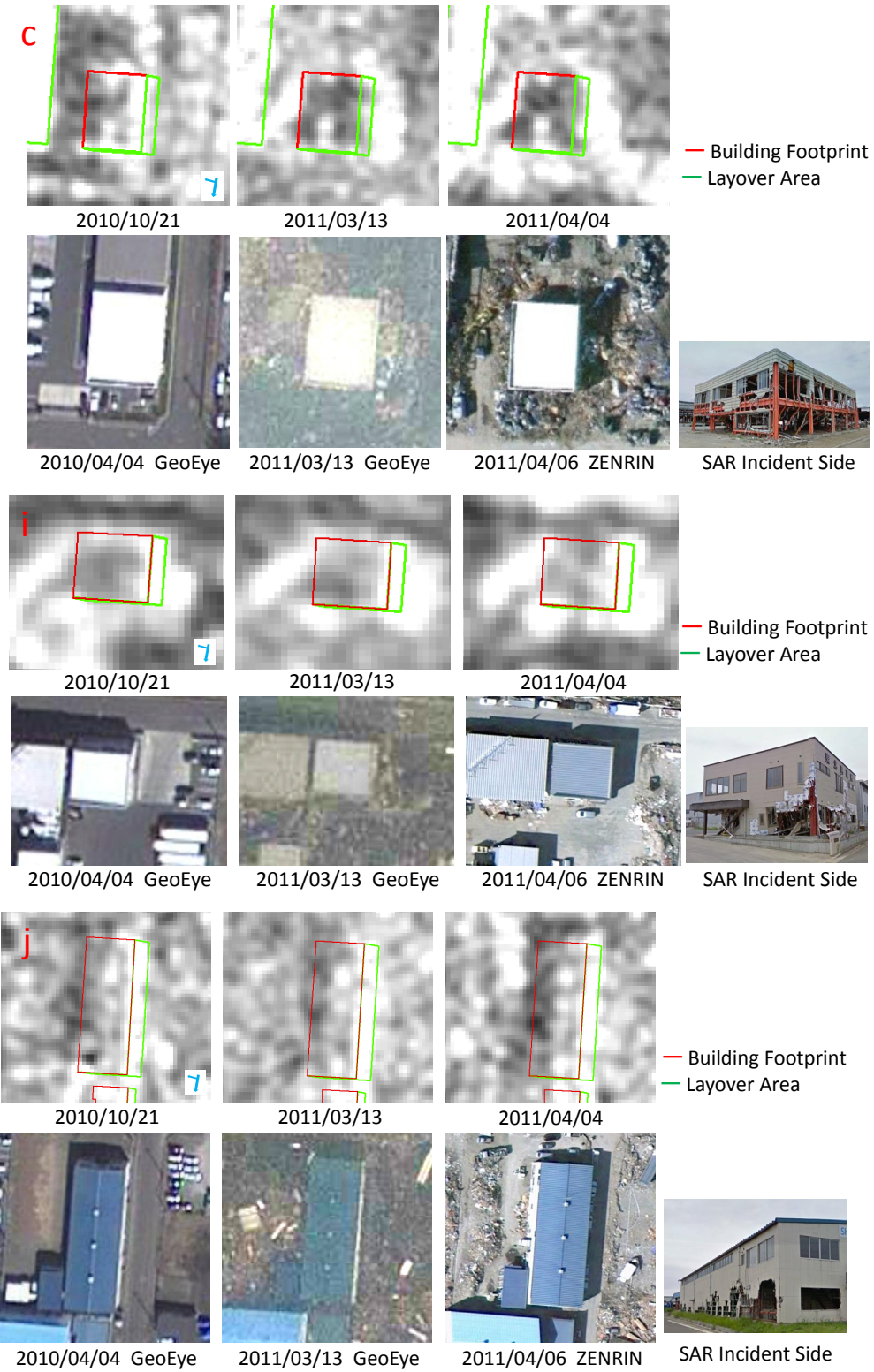
Figure 7. Close-up of the TSX images at the three acquisition dates and the optical images of similar acquisition times for damaged buildings **c**, **i** and **j** in Area **A**. The ground photo of SAR reflection side of each building extracted from Google Street View was also shown.
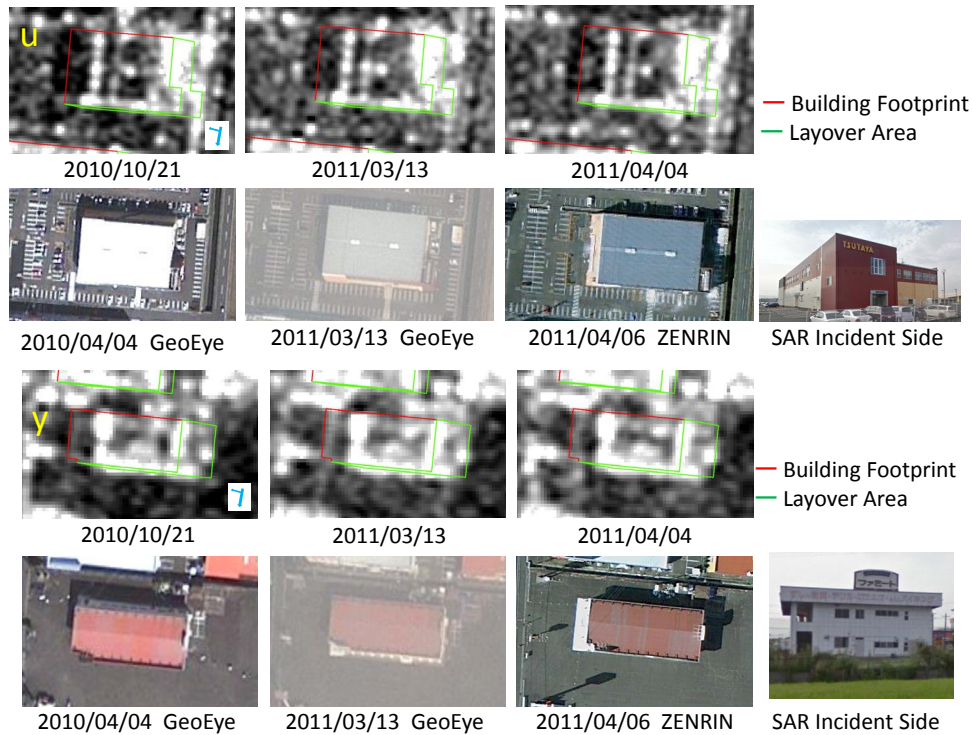
Figure 8. Close-up of the TSX images at the three acquisition dates and the optical images of similar acquisition times for damaged buildings **u** and **y** in Area **B**. The ground photo of SAR reflection side of each building extracted from Google Street View was also shown.

From the detailed observation of damaged and non-damaged buildings at their SAR reflection side faces, the backscatter coefficient in the layover area is considered to be a good indicator to judge the damage status of building side-walls. More examples to verify this view will be provided elsewhere.

5. CONCLUSIONS

Building damage such as to side-walls or mid-story collapse is often overlooked in optical satellite images because the upper surfaces of buildings do not change too much in the vertical view. Hence, the use of high-resolution SAR intensity images is considered with the aid of side looking nature of SAR. In the 2011 Tohoku, Japan earthquake, a large number of buildings were collapsed or severely damaged due to tsunami attack. One of the important aspects of tsunami effects on buildings is that the damage is concentrated to their side-walls and lower stories, which is difficult to observe from vertical images. Thus this paper proposes the method to detect this kind damage from the change in a layover area of an individual building in high-resolution SAR images.

Multi-temporal TerraSAR-X images covering the Sendai-Shiogama Port were employed to detect building damage due to tsunamis after the earthquake. The backscattering coefficients in layover areas of individual buildings were extracted and then, the average values of them were calculated for the pre- and post-event SAR images. Comparing these values, the average value was seen to reduce for damaged buildings in the post-event images due to the reduced backscatter from building side-walls. On the contrary, no much change was seen for most of non-damaged buildings. This example indicates the usefulness of high-resolution SAR images to detect severe damage to building side-walls from the changes of the backscattering coefficient in layover areas.

REFERENCES

[1]   Yamazaki, F., Yano, Y., and Matsuoka, M., "Visual Damage Interpretation of Buildings in Bam City Using QuickBird Images Following the 2003 Bam, Iran, Earthquake," *Earthquake Spectra*, 21(S1), S329-S336 (2005).

[2]   Ghosh, S., Huyck, C, K., Greene, M., Gill, S, P., Bevington, J., Svekla, W., DesRoches, R., Onald, R., Eguchi, T. "Crowdsourcing for Rapid Damage Assessment: The Global Earth Observation Catastrophe Assessment Network (GEO-CAN)," *Earthquake Spectra*, 27(S1), S179-S198 (2011).

[3]   Meslem, A., Yamazaki, F., Maruyama, Y., "Accurate evaluation of building damage in the 2003 Boumerdes, Algeria earthquake from QuickBird satellite images," *Journal of Earthquake and Tsunami*, 5(1), 1-18 (2011).

[4]   Miura, H., Midorikawa, S. and Kerle, N.: "Detection of Building Damage Areas of the 2006 Central Java, Indonesia Earthquake through Digital Analysis of Optical Satellite Images, " *Earthquake Spectra*, 29(2), 453-473 (2012).

[5]   Maruyama, Y., Yamazaki, F., Matsuzaki, S., Miura, H., Estrada, M., "Evaluation of Building Damage and Tsunami Inundation Based on Satellite Images and GIS Data Following the 2010 Chile Earthquake," *Earthquake Spectra*, 28(S1), S165-S178 (2012).

[6]   Iwasaki, Y., and Yamazaki, F., "Detection of building collapse from the shadow lengths in optical satellite images," *Proc. 32nd Asian Conference on Remote Sensing*, Taipei, Paper No. 202, CD-ROM, 6p (2011).

[7]   Brunner, D., Lemoine, G., and Bruzzone, L., "Earthquake damage assessment of buildings using VHR optical and SAR imagery," *IEEE Transactions on Geoscience and Remote Sensing*, 48(5), 2403-2420 (2010).

[8]   Miura, H. and Midorikawa, S., "Preliminary Analysis for Building Damage Detection from High-Resolution SAR Images of the 2010 Haiti Earthquake," *Joint Conference Proceedings of 9th International Conference on Urban Earthquake Engineering and 4th Asia Conference on Earthquake Engineering*, Paper No.01-212 (2012).

[9]   Uprety, P., Yamazaki, F., "Detection of Building Damage in the 2010 Haiti Earthquake using High-Resolution SAR Intensity Images, " *Journal of Japan Association for Earthquake Engineering*, 12(6), Special Issue, 21-35 (2012).

[10] Liu, W., Yamazaki, F., Gokon, H., and Koshimura, S., "Extraction of Tsunami-Flooded Areas and Damaged Buildings in the 2011 Tohoku-Oki Earthquake from TerraSAR-X Intensity Images," *Earthquake Spectra*, 29(S1), S183-S200 (2013).

[11] Liu, W., Yamazaki, F., "Building height detection from high-resolution TerraSAR-X imagery and GIS data," *Proceedings of 2013 Joint Urban Remote Sensing Event*, Sao Paulo, Brazil, CD-ROM, 33-36 (2013).

[12] Geospatial information Authority of Japan. http://www.gsi.go.jp/BOUSAI/h23_tohoku.html

[13] Liu, W., and Yamazaki, F., "Detection of crustal movement from TerraSAR-X intensity image," *IEEE Geoscience and Remote sensing Letters*, 10(1), 199-203 (2013).

[14] Liu, W., Yamazaki, F., Nonaka, T., and Sasagawa, T., "Detection of three-dimensional crustal movements due to the 2011 Tohoku, Japan earthquake from TerraSAR-X intensity images," *Proceedings of SPIE*, Vol. 8524, Land Surface Remote Sensing, 85240Z, CD-ROM, 10p (2012).

[15] Lopes, A., Touzi, R., and Nezry, E., "Adaptive speckle filters and scene heterogeneity," *IEEE Transactions on Geoscience and Remote Sensing*, 28(6), 992–1000 (1990).

[16] Brunner, D., Lemoine, G., Bruzzone, L., and Greidanus, H., "Building Height Retrieval From VHR SAR Imagery Based on an Iterative Simulation and Matching Technique," *IEEE Transactions on Geoscience and Remote Sensing*, 48(3), 1487-1504 (2010).

[17] Ferro, A., Brunner, D., Bruzzone, L., and Lemoine, G., "On the Relationship Between Double Bounce and the Orientation of Buildings in VHR SAR Images," *IEEE Geoscience and Remote Sensing Letters*, 8(4), 612-616 (2011).

[18] Pichel, W.G., Clemente-Colon, P., Wackermanm C.C., Friedman, K.S., "Ship and wake detection, "NOAA SAR Marine Users Manual," Chapter 12, 277-304.
    http://www.sarusersmanual.com/ManualPDF/NOAASARManual_CH12_pg277-304.pdf